# Modelling Static Field Induced Torque on Simplified Medical Devices


Xiao Fan Ding [1], W. B. Handler [1], and B. A. Chronik [1]

[1] The xMR Labs, Department of Physics and Astronomy, Western University, London ON, Canada

Contact: xding57@uwo.ca


## INTRODUCTION

ASTM International is an internationally recognized organization for producing standards. Their most recent standard regarding static field ($\mathbf{B_0}$) induced torque on medical implants was published in 2017 and consists of five test methods [1,2]. Two out of the five aim to quantify the torque induced but neither by computational means [1]. Using stainless-steel (SS) rods as simplified devices, results from a finite element method (FEM) model were compared with measured values at a scanner to determine the feasibility of using FEM to calculate induced torque. This study aims to provide preliminary results for computational medical implant testing.

## METHODS

### Experimental Setup

Sixteen rods were machined and measured for induced torque at a 3 T scanner using the *Pulley Method* published by ASTM International (**Fig.1**). The rods were made of SS304 and 306 with diameters of 0.64 and 1.27 cm and lengths 3, 5, 7, and 9 cm

The rods were placed into a rotating holder the length parallel to $\mathbf{B_0}$. A thread connected the holder to a force gauge which could only move in one direction. As the force gauge pulled away, the rods would rotate away from its initial position. The axis of rotation coincided with the centre of each rod. A torque induced on the rods would cause them to reorient with $\mathbf{B_0}$ which was measurable by the force gauge as tension in the thread. The peak force during a full rotation was used to calculate the peak torque.

### Computational Setup

In COMSOL Multiphysics (COMSOL Inc., Sweden), an FEM solver, a cubic simulation domain was made into which cylinders with dimensions identical to the machined SS rods were placed. The cylinders were defined solely by the magnetic susceptibility, $\chi$. Two physics solvers were used to calculate the $\mathbf{B}$ inside and outside of the cylinders the spatial gradient of the magnetic flux densities, $\nabla\mathbf{B}$. The magnetic force, $\mathbf{F_m}$, could then be calculated by the equation below [3].

$$\mathbf{F_m} = \frac{\chi dV}{\mu_0(1+\chi)}(\mathbf{B}\cdot\nabla)\mathbf{B} \tag{1}$$

In equation (1), $\mu_0$ is the vacuum permeability and $dV$ is the volume of each element. The torque induced on each simulated cylinder, $\boldsymbol{\tau}$, was calculated by summing up the torque on each element at a distance, $r$, from the center of the cylinder (**Fig 2**).

$$\boldsymbol{\tau} = \mathbf{F_m} \times \mathbf{r} \tag{2}$$

The cylinders are rotated in the cubic domain just as the rods would when measured at the scanner.

## EXPERIMENTAL / NUMERICAL SETUP

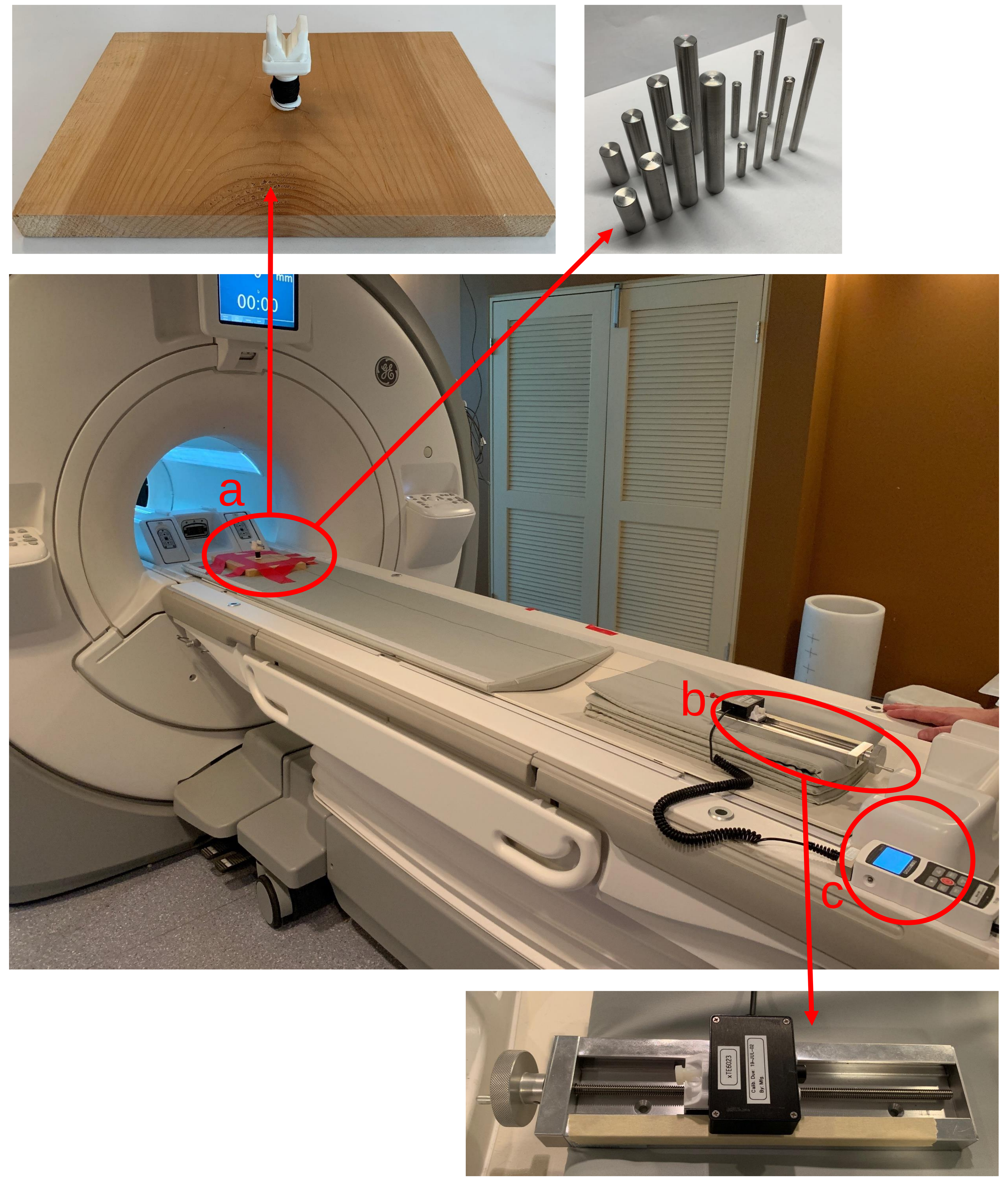


**Fig.1:** Experimental setup in the scanning room. The patient bed was used to move the rotating apparatus holding the test rods into magnetic isocentre, the region where the field is most uniform. a) The rotating apparatus consisted a wooden base and a rod holder designed to hold the two diameters of the rods. A thread extends from the holder to the force gauge. b) Force gauge mounted on a linear displacement track operated by a crank. c) Monitor connected to the force gauge displaying the peak reading.

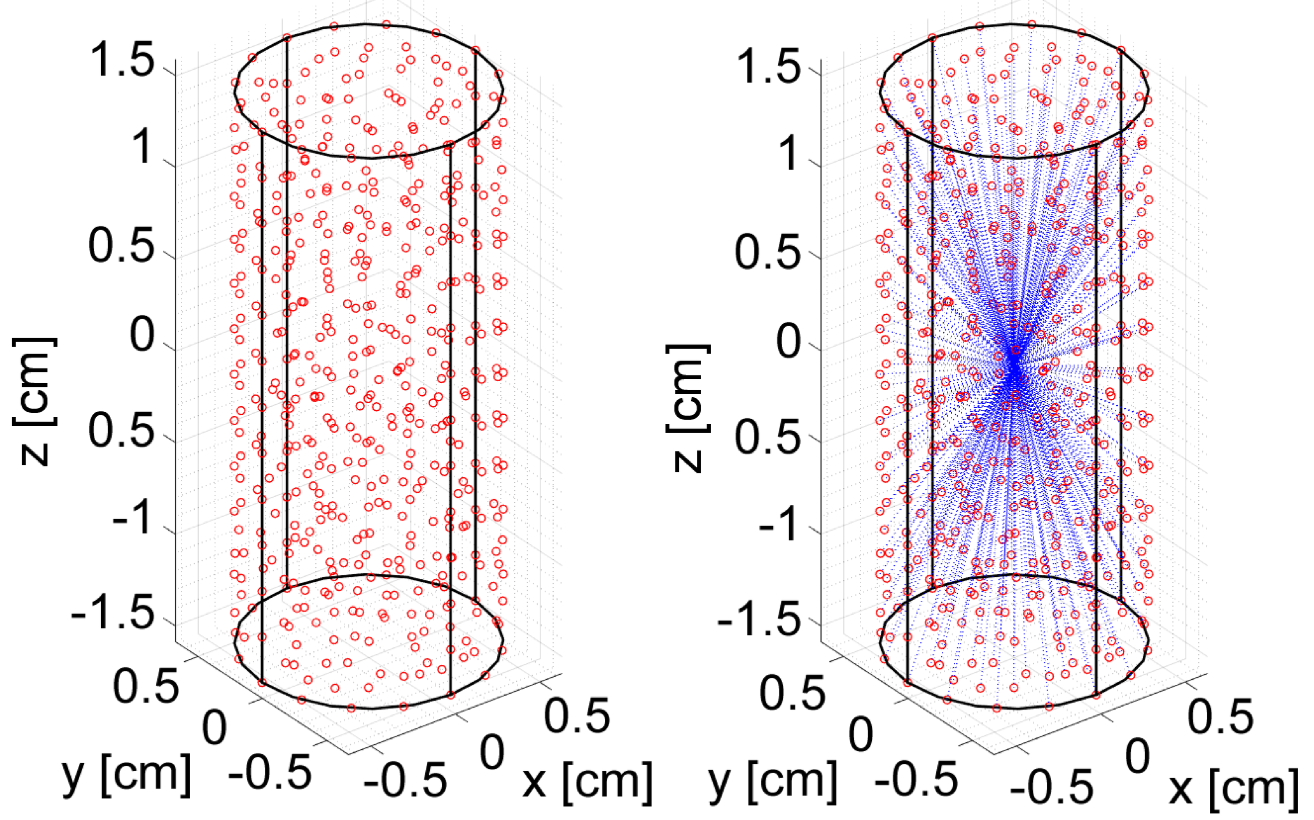


**Fig.2:** Using the 3 cm long and 1.27 cm thick cylinder as an example. The left shows the position of each element (red circles) exported from COMSOL. The right shows a dotted blue line drawn from each element to the centre of the cylinder. At each position, the $\mathbf{B}$, $\nabla\mathbf{B}$, and $dV$ are known. Equations 1 and 2 are then used to calculate the torque induced on the cylinder.

## RESULTS

**Tab.1:** Summary of measured torque at the scanner, the FEM simulated torque, and their percent difference. Since the sixteen rods were cut from four pieces of raw material (two grades of steel at two diameters), the value grouped placed into those categories.

| | Length [cm] | Measured [mNm] | Simulated [mNm] | % diff |
|---|---|---|---|---|
| SS316 $d = 1.27$ cm $\chi = 5026 \pm 34$ ppm | 3 | $0.133 \pm 0.018$ | 0.134 | 0.752 |
| | 5 | $0.307 \pm 0.018$ | 0.301 | 1.954 |
| | 7 | $0.444 \pm 0.019$ | 0.452 | 1.802 |
| | 9 | $0.614 \pm 0.021$ | 0.612 | 0.326 |
| SS304 $d = 1.27$ cm $\chi = 12246 \pm 207$ ppm | 3 | $0.772 \pm 0.016$ | 0.789 | 2.202 |
| | 5 | $1.710 \pm 0.027$ | 1.788 | 4.561 |
| | 7 | $2.787 \pm 0.040$ | 2.677 | 3.947 |
| | 9 | $3.728 \pm 0.052$ | 3.643 | 2.280 |
| SS316 $d = 0.64$ cm $\chi = 5501 \pm 79$ ppm | 3 | $0.052 \pm 0.002$ | 0.053 | 1.923 |
| | 5 | $0.105 \pm 0.004$ | 0.103 | 1.905 |
| | 7 | $0.145 \pm 0.005$ | 0.141 | 2.759 |
| | 9 | $0.168 \pm 0.006$ | 0.175 | 4.167 |
| SS304 $d = 0.64$ cm $\chi = 12542 \pm 128$ ppm | 3 | $0.272 \pm 0.008$ | 0.274 | 0.735 |
| | 5 | $0.515 \pm 0.012$ | 0.538 | 4.466 |
| | 7 | $0.739 \pm 0.016$ | 0.732 | 0.947 |
| | 9 | $0.936 \pm 0.018$ | 0.912 | 2.564 |

## DISCUSSION and CONCLUSION

From **Tab.1**, the percent difference between the measured and simulated torques was less the 5%. The calculated $\chi$ for the four pieces of raw material were all within accepted ranges which is 1000-20000 ppm for stainless steel. SS316 is more precisely known to be between 3520-6700 ppm [4].

**This method requires further validation using better characterized material in terms of $\chi$. Current candidates are grades of cobalt-chrome (700-1500 ppm) and titanium (200 ppm) which are also common materials for implants [5].**

The model as is now is seen to be self-consistent internally and given this self-consistency, FEM models would provide an effective tool for efficient and systematic testing of medical implants. With further models involving greater geometric complexity, the use of computational testing alongside experimental measurements may minimize the number of measurements required for large groups of implants. Rather than testing every configuration, first a model can identify the worst-case and through experimentation, conservative limits can be established for the group as a whole.

## REFERENCES


1. ASTM F2213-17 (2017)
2. Woods, T. O. (2007) *J Magn Reson Imaging*, 26, 1186–1189
3. Nyenhuis, J. A. et al. (2005) *IEEE T Device Mat Re*, 5(3), 467–480
4. Schenck, J. F. (1996). *J Med Phys*, 23(6), 815–850
5. Starcukova J. et al. (2008) *Dent. Mater*, 24, 715-728


## ACKNOLEDGEMENTS


The authors would like to acknowledge the following sources of funding.